LOW-DENSITY–FOAM SHELLS

R. C. Cook *S. A. Letts*

G. E. Overturf, III *S. M. Lambert**

G. Wilemski *D. Schroen-Carey***

Introduction

Future inertial confinement fusion (ICF) targets at the University of Rochester Laboratory for Laser Energetics and at Lawrence Livermore National Laboratory's (LLNL's) planned National Ignition Facility will require 1- to 2-mm-diam spherical organic-polymer shells, each having an 80- to 100-μm-thick cryogenic liquid or solid layer of deuterium–tritium (DT) on its inside surface.[1,2] A potential means of fulfilling this requirement is to line the inside of the plastic capsule with a layer of low-density (~50 mg/cm^3), low-atomic-number foam to help support and symmetrize the fuel.[3] The foam layer also provides the opportunity to dope the DT fuel, which permeates it, with mid-*Z* elements incorporated in the foam that may be useful in providing spectroscopic diagnostics of the implosion.[4,5] In the case of solid DT layers, Collins[6] has shown that DT ice grown on top of foam has a smoother surface finish, presumably because the small cell size of the foam leads to more finely grained crystal sizes. This paper describes fabrication of this inner foam mandrel via the microencapsulation of resorcinol–formaldehyde (RF) aerogel, a foam material developed at LLNL during the past decade for defense and commercial purposes.[7]

Preparation of foam shells by microencapsulation was first developed by Takagi et al.[8–12] using a methacrylate-based chemistry. Shells of this type, filled with cryogenic liquid D_2, have been used in the Japanese ICF program.[10] In that scheme, an aqueous drop is enclosed in an immiscible organic-solvent shell that contains an approximately 5% concentration of a multifunctional methacrylate monomer; this compound drop is, in turn, submerged in an aqueous phase. After the compound drop is formed, a polymerization reaction is initiated in the organic phase to create a cross-linked polymer network (gel) that occupies the volume of the organic phase and provides a solid, gelatin-like state to ensure stability. When polymerization is complete, the water core and the organic solvent permeating the gel are exchanged with a mutually miscible solvent, which is then replaced with liquid CO_2. Dry foam shells are obtained by removing the CO_2 as a supercritical fluid. This drying route is necessary because standard air-drying would cause the foam's very fine cell structure to collapse due to surface forces associated with the vapor/liquid interface. Because the initial organic phase had only approximately 5% solids, the resulting foam has a density of approximately 50 mg/cm^3 (full density is approximately 1 g/cm^3).

This work[8–12] and subsequent work performed at LLNL on methacrylate-based foam shells[13] revealed two important features of the encapsulation technique:

- The polymerization and related gelation of the shell phase must occur quickly to stabilize the inherently unstable compound drop.
- The densities of the inner aqueous droplet and of the nonaqueous shell phase containing the polymerizable compound must be carefully matched to eliminate buoyancy effects that can further destabilize the compound drop and lead to nonuniform shell-wall thickness.

The impetus to pursue RF aerogel shells was realizing an optical transparency considerably greater than that of methacrylate-based foams.[14] The opacity of methacrylate foams is due primarily to the scattering of light by the relatively large (i.e., 1- to 3-μm) cell structure.[15] RF aerogel, on the other hand, has a cell size of approximately 0.1 μm and is therefore significantly more transparent. This allows us to optically monitor the state of the cryogenic DT that fills the shell and, most importantly, to measure the surface finish of the inside DT ice layer, a critical parameter for capsule performance.[1,2]

* Soane Technologies, Hayward, CA
** W. J. Schafer Associates, Livermore, CA

The preparation of RF foams differs considerably from that of methacrylate-based foams, and these differences profoundly affect the encapsulation process. One important difference is that the typical gelation time of conventional RF aerogel formulations is many hours.[7,16–21] Because successful encapsulation is possible only if gelation of the shell phase occurs within 15 to 20 minutes, a means of accelerating the gelation—that can maintain the desired foam properties (e.g., transparency and low density)—is needed. Another important difference is that, in the case of the RF system, polymerization occurs in an aqueous medium rather than in an organic (oil) medium. As a result, an oil-in-water-in-oil system, rather than the water-in-oil-in-water system used for methacrylate foam shells, is needed to create RF aerogel shells.

RF Aerogel Chemistry

The use of RF resin chemistry to form low-density microcellular materials was pioneered by Pekala et al.[7,16–21] In basic aqueous solutions at elevated temperatures (60–95°C), resorcinol and formaldehyde react to form cross-linked, nanometer-sized particles. After the initial particle-formation and -growth stage, which can take several hours, the colloidal particles begin to aggregate and assemble into a stiff, interconnected structure locally resembling a string of pearls that fills the original volume of the aqueous solution. This process of particle growth, followed by aggregation and gelation, is shown schematically in Figure 1.

RF formulations are characterized by three quantities related to the initial composition of the aqueous solution:

1. The first is the molar ratio of formaldehyde to resorcinol (F/R). A ratio of 2 has been used in all previous studies,[7,16–21] but we have investigated the effect of increasing it to 3. Increasing F/R should increase the average number of reactions per resorcinol and, ultimately, the degree of cross-linking.
2. The second quantity is the molar ratio of resorcinol to catalyst (R/C). The catalyst in this reaction is sodium carbonate, which activates a small fraction of the resorcinol molecules to act as sites for the growth of RF particles. Reducing R/C (i.e., increasing the catalyst concentration) produces more particles of smaller size. Investigation here is limited to R/C ratios of 100 and 200 because it is known that these yield the lowest density and most optically transparent foams.[7,16–18]
3. The last quantity is the theoretical dry-foam density, which is determined from the concentration of polymerizable reactants (resorcinol and formaldehyde) in the initial aqueous solution. A solution containing a combined 5 wt% of resorcinol and formaldehyde will have a theoretical density of approximately 50 mg/cm^3. Due to some shrinkage of the gel upon drying, actual foam densities are usually slightly higher than the theoretical densities. We have worked primarily with RF formulations that produce foams with theoretical densities of 50 and 75 mg/cm^3.

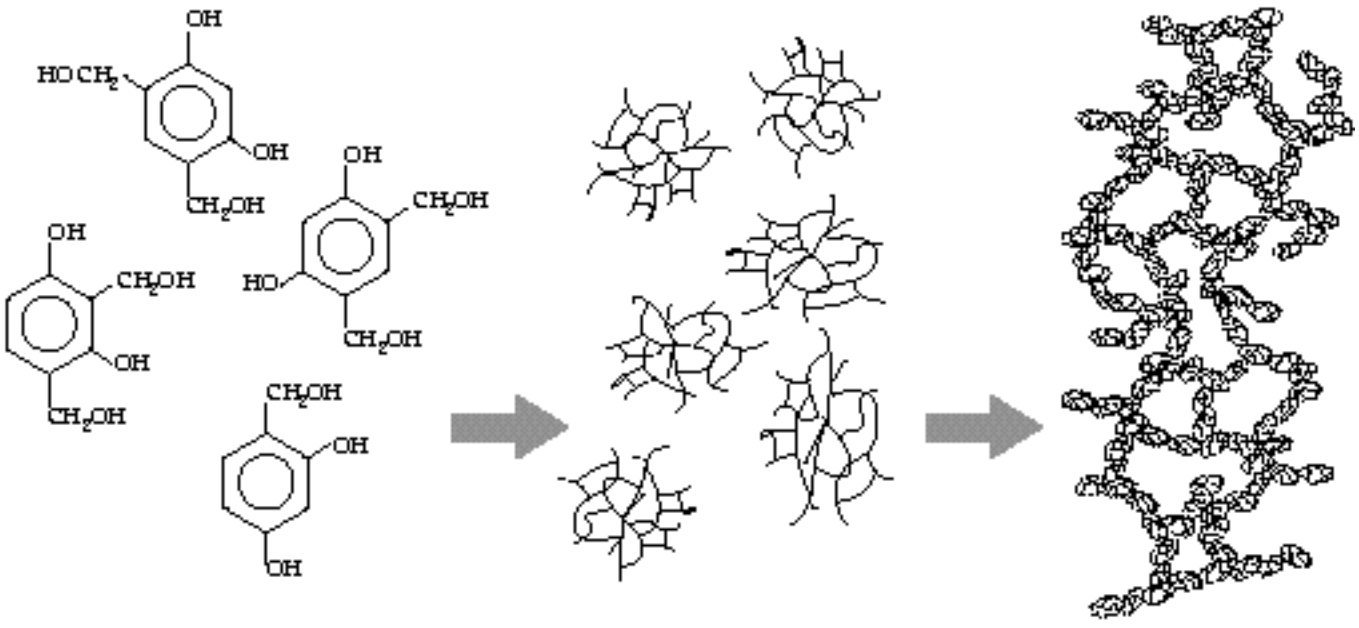

FIGURE 1. Left: Substituted resorcinol is formed by the initial reaction between resorcinol and formaldehyde. Center: These substituted resorcinol moities react to form cross-linked clusters. Right: Finally, the cross-linked clusters condense into extended "chain-of-pearls" cross-linked molecules, forming a gel-like material. (02-32-0688-1671pb01)

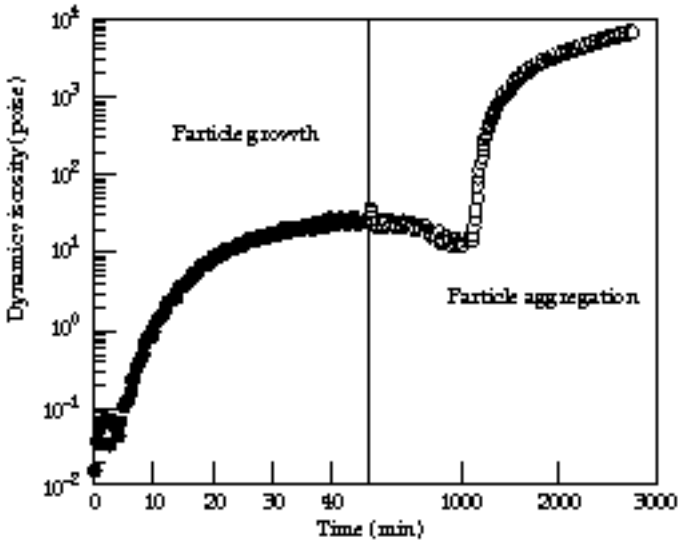

FIGURE 2. Dynamic viscosity of an RF solution (30 mg/cm^3 theoretical foam density, F/R= 2, R/C= 100) at 70°C. The first regime corresponds to particle growth. The second regime corresponds to particle aggregation to form the stiff gel. Note change in time scale between regimes on the horizontal axis. From Letts et al.[18] (70-00-0197-0149pb01)

Letts et al.[18] have shown, by dynamic viscosity measurements, that the base-catalyzed RF reaction at 70°C is initially dominated by particle growth that typically ceases after approximately 1 h. In Figure 2, this is illustrated by the dynamic vicosity's initial rise and plateauing at a relatively low value. At some point many hours later (note change in scale), a second large increase in the dynamic viscosity signals the aggregation of particles to form a stiff gel. Titration measurements[19] show that most of the formaldehyde is consumed within the first half hour. These results, coupled with light scattering studies,[20,21] provide convincing evidence that particle growth is completed well before aggregation begins.

We have found that the reactions taking place during the particle-growth stage slowly increase the acidity of the reacting medium. After particle growth has stopped due to the depletion of formaldehyde, the acid-catalyzed reactions between the surfaces of particles create links between particles to form chemical bridges. Nuclear magnetic resonance studies[17] support this difference between intra- and interparticle chemical structures. Because the solution is typically only slightly acidic after particle growth, aggregation proceeds at a slow rate. We reasoned that artificially lowering the pH by adding acid should more rapidly aggregate the particles to the point of gelation.

We confirmed this hypothesis experimentally. Figure 3 shows the effect on the dynamic viscosity of increasing the acidity by a factor of 10 by adding benzoic acid after 1 h of conventional base-catalyzed reaction. After a short period, the dynamic viscosity rapidly increases and plateaus at gel-like values. This result has led to the two-step procedure for preparing RF gels that is outlined in Figure 4. First, the reactants are mixed together and base-catalyzed at 70°C for 1 h. The solution is then cooled for several minutes in an ice-water bath, and benzoic acid is added to increase the acidity. The compound droplets are then formed in a 70°C oil bath, as will be described subsequently, and this increase in temperature of the now acid-catalyzed RF solution results in rapid gelation of the shells.

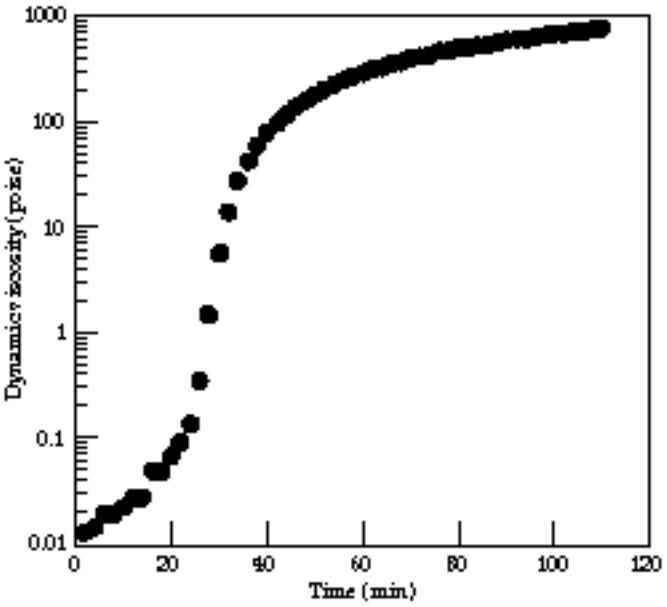

FIGURE 3. Dynamic viscosity of an RF solution (50 mg/cm^3 theoretical foam density, F/R= 2, R/C =200) at 70°C that has been spiked with 0.026 wt% benzoic acid following 1 h conventional base-catalyzed reaction. (70-00-0197-0151pb01)

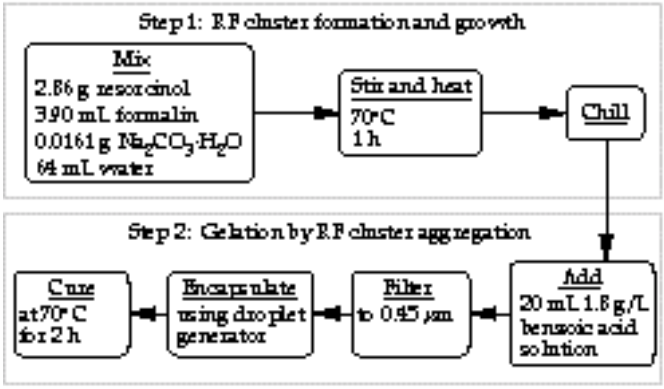

FIGURE 4. The two-step process for preparing acid-accelerated RF gels (50 mg/cm^3 theoretical foam density, F/R= 2, R/C=200). (70-00-0197-0152pb01)

To optimize this two-step RF polymerization process, we studied the effects of modifying the R/C ratio, the length of the initial base-catalysis period, and the amount of benzoic acid added. For all solutions, $F/R = 2$. The goals of this study were to decrease the gelation onset time (some indication of how long it takes the gel to set and thus stabilize the compound droplet) and to maximize the dynamic viscosity of the gel after curing for 2 h (to give an indication of the strength and stiffness of the gelled material).

Figure 5 shows the effect of varying the acid content on the dynamic viscosity of formulations with different values of R/C. Both the $R/C = 100$ and the $R/C = 200$ solutions were base-catalyzed for 1 h. For both values of R/C, increasing the acid concentration set the gels more rapidly and increased the plateau viscosity. Understanding the effect of changing R/C for a given amount of benzoic acid is not as straightforward. R/F solutions become more basic as R/C is decreased. Because of the increased basicity, more of the added acid will be used to neutralize the carbonate rather than to promote aggregation. As a result, a given amount of acid will be less effective in promoting gelation in low-R/C solutions than it will in high-R/C solutions. This is most evident in Figure 5(a) when 0.036 g benzoic acid is added; as R/C decreases, the gelation onset time begins later. Despite delay in the onset of gelation, gels with lower R/C plateau at a slightly higher viscosity. As shown in Figure 5(b), with solutions having higher acid contents, the effect of differences in R/C become less distinguishable.

Figure 6 shows the effect of varying the length of the initial base-catalysis period. The viscosity behavior is significantly affected within the first hour; after 0.5 h, particle growth is probably still occurring. The increases in gelation rate and plateau viscosity when base-catalysis time is extended beyond 1 h are probably due to continued intraparticle cross-linking and the start of some aggregation before acid addition. Increasing the base-catalysis time has an effect similar to that of increasing acid content; hence, for longer base-catalysis periods, less acid is needed to accelerate gelation.

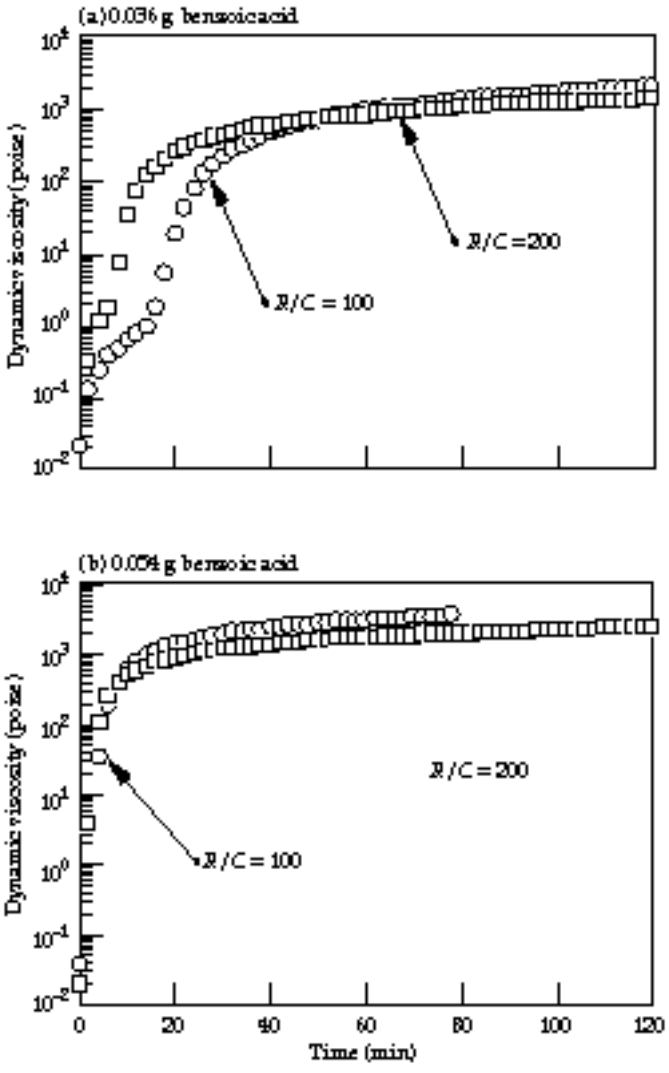

FIGURE 5. Dynamic viscosity of RF solutions (50 mg/cm^3 theoretical foam density, $F/R = 2$) during cure at 70°C as a function of R/C and the amount of benzoic acid added. (70-00-0197-0153pb01)

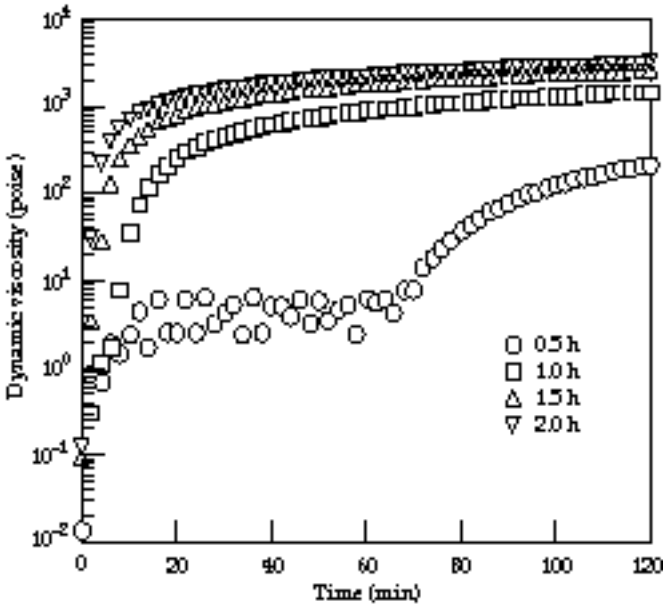

FIGURE 6. Dynamic viscosity of RF solutions (50 mg/cm^3 theoretical foam density, $F/R = 2$, $R/C = 200$, 0.036g benzoic acid added) during cure at 70°C as a function of base-catalysis time. (70-00-0197-0154pb01)

Swelling of RF Gels in Isopropanol

To produce dry foams, one must replace the water solvating the gel with isopropanol (IPA) before subsequently replacing IPA with liquid CO_2, which is then supercritically vented. IPA was chosen as the intermediate solvent because it is miscible with both water and liquid CO_2. When gels were cured (reacted) for 2 h and then exchanged into IPA, we observed macroscopic swelling (which is detrimental to useful shell formation) that suggested the material was not sufficiently cross-linked. Because of the colloidal nature of the gel structure, there are two types of cross-links: intraparticle cross-links (within the nanometer-sized particles making up the gel matrix) and interparticle cross-links. Swelling most likely emanates from the former because swelling is indicative of a molecular-level interaction between the polymer and solvent. The most obvious way to increase intraparticle cross-linking is simply to increase the curing time.

Consequently, the degree of swelling of bulk RF gels in IPA was measured as a function of cure time. We also investigated the influence of R/C and F/R on swelling. The results are presented in Figure 7 in terms of the degree of swelling:

$$\frac{\Delta V}{V} \equiv \frac{V_{IPA} - V_W}{V_W} \quad , \tag{1}$$

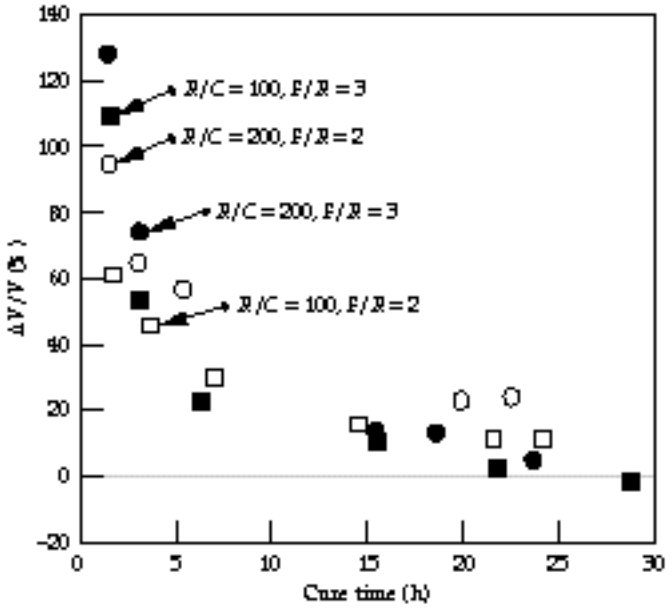

FIGURE 7. Degree of swelling of bulk RF gels (50 mg/cm^3 theoretical foam density) in isopropanol as a function of cure time at 70°C for several combinations of F/R and R/C. (70-00-0197-0156pb01)

where V_W and V_{IPA} are the volumes of the gel piece before (V_W) and after (V_{IPA}) exchanging into IPA. The most important observation was that significant changes in gel dimensions after exchanging into IPA can only be avoided by curing the gel for at least 20 h, rather than the 2 h suggested by the dynamic viscosity measurements. R/C and F/R also influence swelling to a lesser extent. For a given F/R, gels prepared with $R/C = 100$ swell less than gels with $R/C = 200$. Lowering R/C results in the growth of smaller particles, which are probably more cross-linked. For a given R/C and long curing times, swelling can be reduced further by increasing F/R from 2 to 3, which also promotes intraparticle cross-linking.

In summary, this study of RF chemistry, viscometry, and swelling provided important information needed to successfully encapsulate the RF material to form shells. By spiking the RF solutions with an appropriate amount of acid following the base-catalyzed particle-growth stage, the gelation times can be reduced from many hours to less than 20 min. However, although the macroscopic interparticle gel structure gels in minutes, additional annealing of the gel is needed for as long as 20 h to maximize intraparticle cross-linking and thus minimize swelling in the IPA exchange solvent.

Encapsulation Method, Solvents, and Curing

Encapsulation of RF solutions to form a spherical shell is accomplished by using a triple-orifice droplet generator. The generator and compound RF droplets (called preforms) are shown schematically in Figure 8. A preform consists of an interior-oil-phase droplet surrounded by the ungelled aqueous RF solution. This compound drop is formed from two concentric orifices that are inserted into a tube (the third orifice) through which flows a second, exterior-oil phase. The droplets are stripped off the inner orifices by the axial flow of the exterior-oil phase. The delivery tube (10 cm in length) is made of Teflon® to provide a hydrophobic surface that is wetted only by the exterior-oil phase and not by the aqueous RF solution droplets. The diameter of the compound droplet is roughly determined by the diameter of the delivery tube. More precise adjustment of the diameter is achieved by adjusting the exterior-oil-phase flow rate. The shell's wall thickness is determined by the ratio of the interior-oil-phase flow rate to the RF solution flow rate.

The preformed shells flow down the delivery tube into a gently stirred, heated beaker containing approximately 150 mL of the exterior-oil phase. Agglomeration and coalescence of the preforms are reduced by adding surfactant to the exterior-oil phase. Each batch created

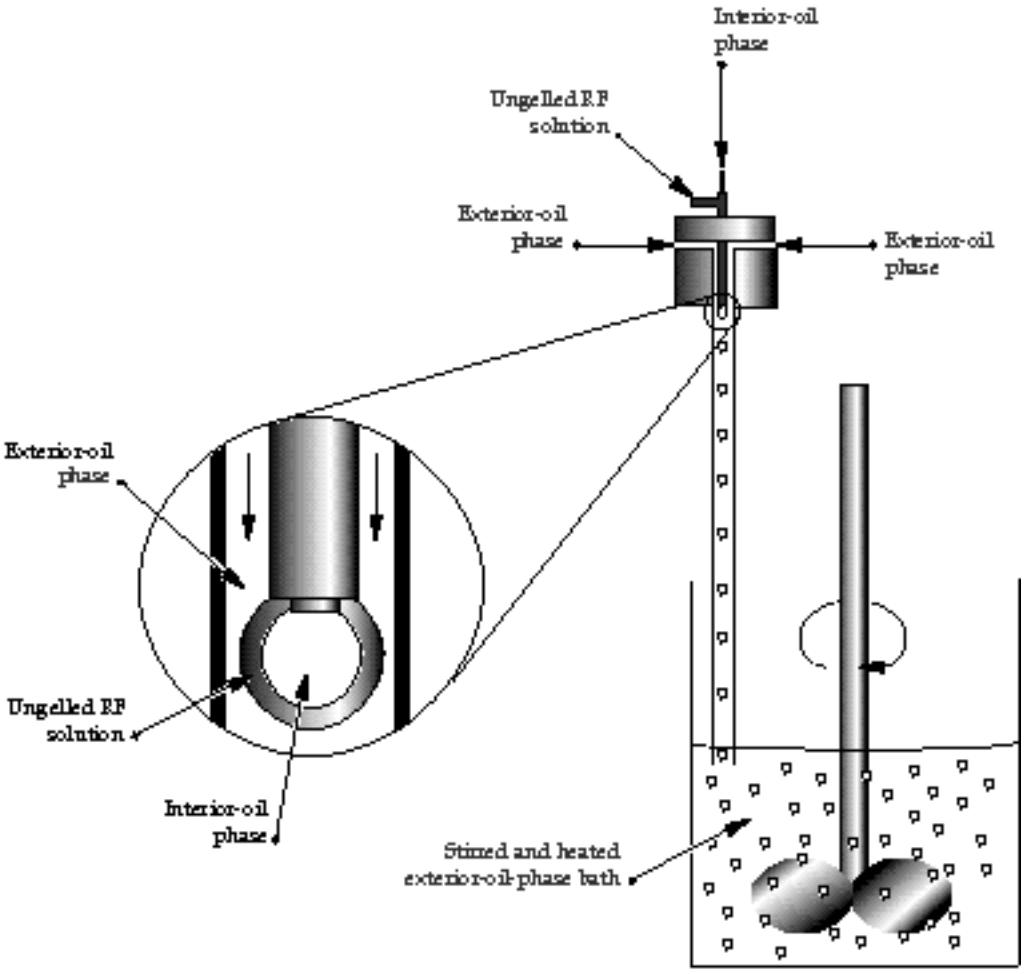

FIGURE 8. Schematic diagram of the triple-orifice droplet generator. (70-00-0197-0157pb01)

by the droplet generator has approximately 200 to 300 shells, of which one-third to two-thirds survive the curing step.

The choice of appropriate interior- and exterior-oil phases was not immediately obvious. The only initial requirements were that they be immiscible with water and that the interior phase be closely matched in density to the aqueous RF phase to minimize wall-thickness nonuniformity due to buoyancy effects. Dibutyl phthalate was chosen initially for the exterior-oil phase because it was used for the preparation of methacrylate foam shells.[12,13] For reasons of density matching, 1-methyl naphthalene was chosen as the interior-oil phase. The density of the exterior-oil phase is also important, but for a different reason: to help keep the compound drops suspended (but not at the surface) without applying vigorous agitation, the density of the exterior-oil phase should be only slightly less than that of the compound drops.

In retrospect, dibutyl phthalate was a poor choice for the exterior-oil phase. Initial results[14] showed that shell walls thinned during cure because of a loss of water from the aqueous phase. This dehydration resulted in shells with foam densities that were two to three times greater than the theoretical foam density. Although dibutyl phthalate is immiscible with water, we found that it, in fact, had enough capacity to dissolve much of the water present in the preformed shells. The solubility of water in dibutyl phthalate at 25°C is 0.46 wt%.[22] The dibutyl phthalate (as received) was determined to already contain 0.12 wt% water. Hence, 150 mL of dibutyl phthalate (a typical bath volume) has the capacity to absorb approximately 0.5 g water, which is about half the water present in 100 compound drops. This situation is exacerbated at the higher temperatures needed to cure the RF gel. Attempts to saturate the exterior-oil phase with water before attempting encapsulation failed because doing so severely reduced the effectiveness of the surfactant and resulted in shell agglomeration.

Using a model for convectively enhanced mass-transfer from an isolated aqueous shell suspended in an agitated nonaqueous solvent, we examined factors that control the transport of water from the shell into the exterior-oil phase. We found that the rate of water lost from the shell can be written as[23]

$$\frac{df}{dt} \quad \frac{k_s T^{2/3} \omega^{1/2}}{\delta \mu^{5/6}} \qquad (2)$$

where f is the fraction of water removed from the shell, t is time, k_s is related to the solubility of water in the oil phase, T is temperature, ω is related to the degree of solution agitation, δ is the shell-wall thickness, and μ is the viscosity of the exterior-oil phase.

Equation (2) points out the desirable properties and processing conditions that help reduce shell dehydration:

- As expected, the rate of water transport out of the shell is directly proportional to the solubility of water in the organic-oil phase.
- Equation (2) suggests we should cure at lower temperatures with reduced agitation.
- Oil phases with higher viscosity will retard water transport out of the shell.

This analysis led us to consider using a grade of mineral oil commonly known as Nujol oil. This fluid has a very low water solubility (0.0038 wt% at 25°C), which is more than two orders of magnitude smaller than that of dibutyl phthalate. It also has a higher viscosity. A major drawback, however, is that its density (0.85 g/cm^3 at 25°C) is too low to keep the shell preforms adequately suspended. This problem can be circumvented by sacrificing some of the higher viscosity of the mineral oil by mixing it with approximately 40 wt% carbon tetrachloride, which has a high density and a comparatively low water solubility (1.59 g/cm^3 and 0.011 wt% at 25°C). We found that shells cured in this oil-phase mixture at 70°C for 1.5 h to 2 h would form stiff-gelled preforms that were significantly less dehydrated than shells cured under the same conditions in dibutyl phthalate. However, although 1.5 h to 2 h is enough time to stabilize and stiffen the shell preforms, we found that water evaporation from the heated system became the dominant mechanism for additional water loss over the remaining 20–22 h of cure needed to maximize intraparticle cross-linking.

To avoid this dehydration of the shells over longer times, the gelled shells were annealed in the configuration shown schematically in Figure 9. After the initial 1.5 h to 2 h of curing, the preforms had hardened enough that agitation was no longer required. Additional carbon tetrachloride was added until the shells floated near the surface. Water was then placed on top of the denser oil phase, saturating it and preventing further dehydration. The beaker was covered and placed in a 70°C constant temperature bath for an additional 20–22 h to finish the cure.

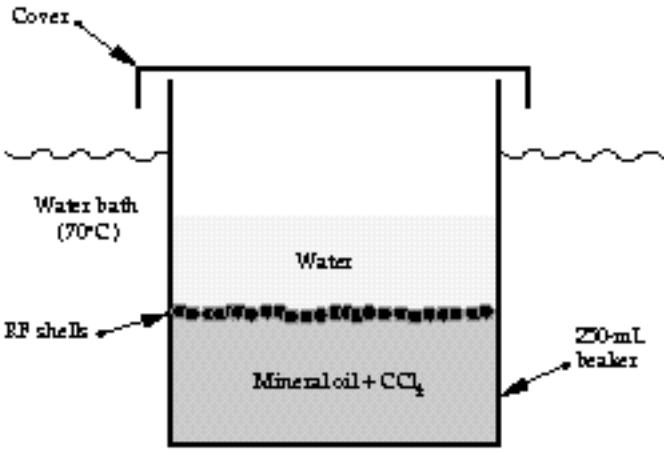

FIGURE 9. Configuration for annealing-gelled RF shells for long periods. (70-00-0197-0158pb01)

Solvent Exchange, Drying, and Characterization

During this final annealing period, the shells eventually sank to the bottom of the beaker because the dense carbon tetrachloride from the exterior-oil phase preferentially permeated the aqueous layer to replace the 1-methyl naphthalene interior-oil phase. This helped separate shells from residual RF debris (broken and collapsed shells), which tends to remain at the oil–water interface; this separation allowed decanting of the water, RF debris, and most of the oil phase, leaving the shells behind. Surviving shells were soaked in IPA to dissolve excess exterior-oil phase, to replace the water solvating the gel, and to replace the interior-oil phase. After numerous exchanges with fresh IPA, the shells were ready to be dried by means of the supercritical drying technique.

The consistency of shell dimensions and wall thickness within a batch is illustrated in Figure 10. The droplet generator has the capacity to make shells that, in IPA, have diameters ranging from 1.6 mm through 2.3 mm and wall thicknesses ranging from 100 μm through 200 μms. The deviations of diameters and wall thicknesses within a batch of shells is typically ±0.03 mm and ±10 μm, respectively.

The measured foam densities of shells were found to be slightly greater than those of bulk RF aerogel samples prepared with the same formulation (shown in Table 1). This is a likely indication that some unavoidable dehydration of the shells by the oil-phase solvents was still occurring. Further, shells and bulk samples prepared with $R/C = 100$ had higher densities

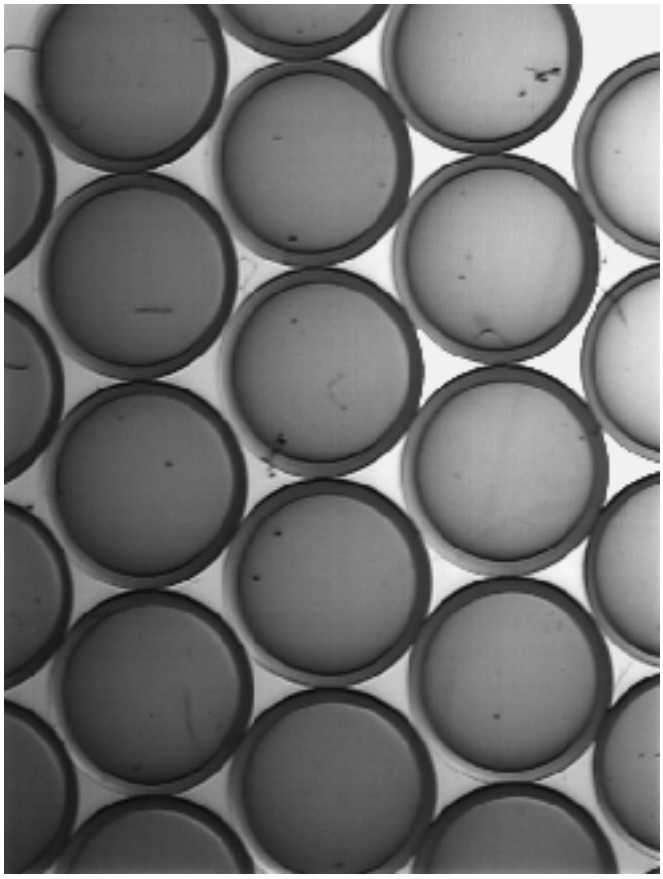

FIGURE 10. A typical batch of RF shells after exchange into isopropanol; for this batch, the average diameter was 2.3 mm, and the average wall thickness was 145 μm. (70-00-0197-0159pb01)

TABLE 1. Measured dry-foam densities of RF shells and bulk RF aerogel as a function of R/C and F/R (the theoretical density of all samples is 50 mg/cm^3).

Sample Description	Measured Density (mg/cm^3)
$R/C = 100$, $F/R = 2$	
Bulk	73
Shells	80
$R/C = 100$, $F/R = 3$	
Bulk	55
Shells	65
$R/C = 200$, $F/R = 2$	
Bulk	47
Shells	64
$R/C = 200$, $F/R = 3$	
Bulk	48
Shells	60

than did samples prepared with $R/C = 200$. This observation is consistent with an earlier finding[7] that $R/C = 100$ gels shrink more upon drying than $R/C = 200$ gels. Lastly, when F/R was increased from 2 to 3, the gels swelled less in IPA. Therefore, with respect to final foam density and reduced dimensional changes during processing, RF formulations with $F/R = 3$ and $R/C = 200$ are optimal.

Dry foam shells were also examined by optical and scanning electron microscopy (SEM). Figure 11 is a photo of a dry shell placed on top of a millimeter scale. This photo clearly demonstrates the optical transparency of the aerogel and provides a visual indication of the uniformity and sphericity of the wall that can be achieved. SEM analyses of a fractured shell wall indicate that the density of the foam is uniform throughout and that the foam shows the same submicrometer cell structure as RF aerogel prepared by conventional means.

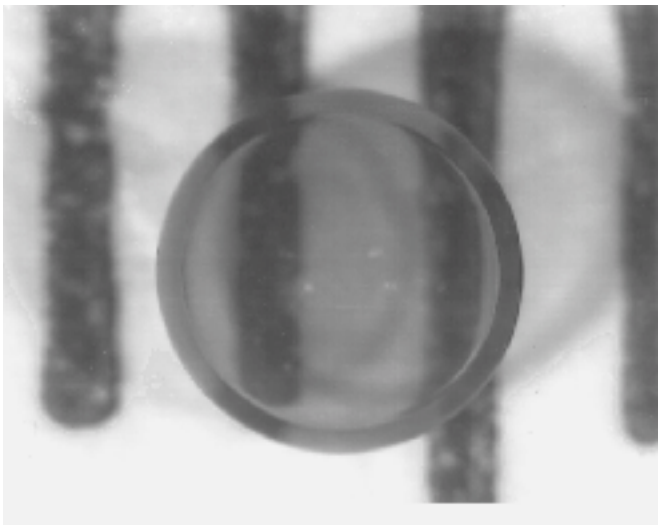

FIGURE 11. Photograph of a dry RF foam shell; diameter is 1.90 mm, wall thickness is 120 μm, and density of the shell is 63 mg/cm^3. (70-00-0197-0160pb01)

Summary

We have successfully developed a process to fabricate hollow spherical shells from low-density RF aerogel. The most notable accomplishments of this work are reduction in gelation time and decreased shell dehydration. The time required to set the macroscopic interparticle gel structure was reduced from several

hours to several minutes by adding acid following the base-catalyzed particle-growth stage. However, additional annealing of the gel for at least 20 h is needed to maximize intraparticle cross-linking and to minimize swelling in exchange solvents. Increasing the molar ratio of formaldehyde to resorcinol from 2 to 3 also helps reduce swelling and reduce the shrinkage of the gel upon supercritical-CO_2 drying. Dehydration of the shells during cure was drastically reduced by prudent selection of immiscible oil phases and by saturating the exterior-oil phase with water during the annealing process. The resulting foam shells have densities that approach their theoretical value and the measured density of bulk aerogel of the same formulation.

When considering the use of these shells as potential fuel containers for ICF experiments, two important issues remain:

- The factors that control shell wall-thickness uniformity must be explored. The only control employed here was density matching, which essentially limited the position of the interior-oil droplet to a random walk within the aqueous RF droplet. We are not cognizant of any naturally occurring centering forces, and artificial ones[24] appear difficult to implement.
- ICF target specifications require that the outside of the shells be coated with a transparent, smooth, full-density polymer layer 5–200 μm thick. We have explored two methods for overcoating shells. The first is deposition of the layer from the vapor phase onto a dry shell using plasma-polymerization techniques;[25–27] in a limited number of experiments, we found that this method produced an unacceptably rough surface. The second method is the use of an interfacial polycondensation technique in the liquid phase (prior to drying); this is similar to that developed by Takagi et al.[10] for methacrylate foam shells. Work in this area has shown some positive results, but additional work is still necessary to meet the surface specifications for the National Ignition Facility.

Acknowledgments

The authors thank Dr. Richard Pekala for useful discussions concerning RF chemistry.

This article is a less technical version of the paper that appears in the *Journal of Applied Polymer Science*.[23]

Notes and References

1. S. W. Haan, et al., *Phys. Plasmas*, **2,** 2480 (1995).
2. S. Lindl, *Phys. Plasmas*, **2,** 3933 (1995).
3. R. A. Sacks and D.H. Darling, *Nucl. Fusion*, **27,** 447 (1987).
4. C. J. Keane, et al., *Rev. Sci. Inst.*, **66**, 689 (1995).
5. C. J. Keane, et al., *J. Quant. Spectrosc. Radiat. Transfer*, **54,** 207 (1995).
6. G. Collins, LLNL Lasers, Livermore, CA, private communication (1995).
7. R. W. Pekala, C. T. Alviso, and J. D. LeMay, "Organic Aeorgels: A New Type of Ultrastructured Polymer," in *Chemical Processing of Advanced Materials*, L.L. Hench and J. K. West, eds., (John Wiley & Sons, NY, 1992), pp. 671–683.
8. C. Chen, T. Norimatsu, M. Takagi, H. Katayama, T. Yamanaka, and S. Nakai, *J. Vac. Sci. Technol. A*, **9,** 340 (1991).
9. M. Takagi, T. Norimatsu, T. Yamanaka, S. Nakai, and H. Ito, *J. Vac. Sci. Technol. A*, **9,** 820 (1991).
10. M. Takagi, M. Ishihara, T. Norimatsu, T. Yamanaka, Y. Izawa, and S. Nakai, *J.Vac. Sci. Technol. A*, **11,** 2837 (1993).
11. T. Norimatsu, C. M. Chen, K. Nakajima, M. Takagi, Y. Izawa, T. Yamanaka, and S. Nakai, *J. Vac. Sci. Technol. A*, **12,** 1293 (1994).
12. M. Takagi, T. Norimatsu, Y. Izawa, and S. Nakai, *MRS Symp. Proc.*, **372,** 199 (1995).
13. D. Schroen-Carey, G. E. Overturf, III, R. Reibold, S. R. Buckley, S. A. Letts, and R. Cook, *J. Vac. Sci. Technol. A*, **13,** 2568 (1995).
14. G. E. Overturf, III, R. Cook, S. A. Letts, S. R. Buckley, M. R. McClellan, and D. Schroen-Carey, *Fusion Tech.*, **28,** 1803 (1995).
15. R. B. Stephens, *Fusion Tech.*, **28,** 1809 (1995).
16. R. W. Pekala, *J. Mat. Sci.*, **24,** 3221 (1989).
17. R. W. Pekala, C. T. Alviso, F. M. Kong, and S. S. Hulsey, *J. Non-Cryst. Solids*, **145,** 90 (1992).
18. S. A. Letts, S. R. Buckley, F. M. Kong, E. F Lindsey, and M. L. Sattler, *Mat. Res. Soc. Symp.*, **177,** 275 (1990).
19. R. W. Pekala, F. M. Kong, *Rev. Phys. Appl. Sup.*, **4,** 24 (1989).
20. P. M. Cotts, R. W. Pekala, *Polym. Preprints*, **32,** 451 (1991).
21. P. M. Cotts, "Static and Dynamic Light Scattering from Solutions and Gels of RF Particles," in *Synthesis, Characterization, and Theory of Polymeric Networks and Gels*, S. M. Aharoni, ed., (Plenum Press, NY, 1992), pp. 41–51.
22. J. A. Riddick, W. B. Bunger, and T. K. Sakano, *Organic Solvents: Physical Properties and Methods of Purification*, (John Wiley & Sons, NY, 1986), p. 442.
23. S. M. Lambert, G. E. Overturf, III, G. Wilemski, S. A. Letts, D. Schroen-Carey, and R. Cook, *J. Appl. Poly. Sci.* **65**, 2111 (1997).
24. C. P. Lee and T. G. Wang, *J. Fluid Mech.*, **188,** 411 (1988).
25. G. W. Collins, S. A. Letts, E. M. Fearon, R. L. McEachern, and T. P. Bernat, *Phys. Rev. Lett.*, **73,** 708 (1994).
26. S. A. Letts, D. E. Miller, R. A. Corley, T. M. Tillotson, and L. A. Witt, *J. Vac. Sci. Technol. A*, **3,** 1277 (1985).
27. S. A. Letts, D. W. Myers, and L. A. Witt, *J. Vac. Sci. Technol. A*, **19,** 739 (1981).